

# Normal-incidence voltage-tunable middle- and long-wavelength infrared photoresponse in self-assembled InAs quantum dots

Zhonghui Chen,<sup>a)</sup> Eui-Tae Kim, and Anupam Madhukar

Nanostructure Materials and Devices Laboratory, Department of Materials Science and Department of Physics, University of Southern California, Los Angeles, Los Angeles, California 90089-0241

(Received 25 June 2001; accepted for publication 7 February 2002)

We report the realization of electron intraband absorption based middle- ( $\sim 5.6 \mu\text{m}$ ) and long- ( $\sim 10 \mu\text{m}$ ) wavelength infrared (IR) photoresponse for normally incident radiation on InGaAs-capped GaAs(001)/InAs quantum dots (QDs) in a  $n-i(\text{QD})-n$  structure. The relative photoresponse in this dual-wavelength structure is tunable up to two orders of magnitude with bias. The full width at half maximum of the long-wavelength IR intraband photocurrent peak at 80 K is as narrow as 8.2 meV.

© 2002 American Institute of Physics. [DOI: 10.1063/1.1467974]

Multicolor and voltage-controlled tunable middle- and long-wavelength (3–14  $\mu\text{m}$ ) infrared (IR) photodetectors are attractive because of their potential for applications in terrestrial and space-borne sensors and imaging systems. Significant progress has been made in the demonstration of multicolor and voltage-controlled tunable quantum-well intraband IR photodetectors.<sup>1</sup> Self-assembled semiconductor quantum dots (QDs) (Ref. 2) are particularly attractive candidates for middle- and long-wavelength IR photodetectors due to their intrinsic sensitivity to normally incident IR light,<sup>3</sup> and the longer lifetime of excited electrons due to greatly suppressed electron–phonon scattering.<sup>4</sup> Encouraging results have been reported on normal-incidence intraband GaAs(001)/InAs/GaAs and GaAs(001)/InGaAs/GaAs quantum-dot IR photodetectors (QDIPs) in both  $n-n(\text{QD})-n$  (Refs. 5 and 6) and  $n-i(\text{QD})-n$  (Ref. 7 and 8) configurations. In this letter, we report on normal-incidence  $n-i(\text{QD})-n$  QDIPs based on GaAs(001)/InAs pyramidal islands capped with a InGaAs strain-relieving layer that give rise to voltage-controlled tunable simultaneous middle- and long-wavelength intraband IR photoresponse at 80 K.

The QDIP samples, shown schematically in Fig. 1(a), were grown on semi-insulating GaAs(001)  $\pm 0.1^\circ$  substrates via solid-source molecular-beam epitaxy (MBE). The structures comprise Si-doped ( $10^{17}$ – $10^{18}/\text{cm}^3$ ) bottom and top GaAs layers with an undoped active QD region in between. The active region consists of a stack of five QD layers, each made of nominal 2.5 ML InAs pyramidal islands. GaAs(001)/InAs was deposited at the growth rate of 0.0625 ML/s at 500  $^\circ\text{C}$  under an As pressure of  $7 \times 10^{-6}$  Torr. On the islands so formed, 30 ML  $\text{In}_{0.15}\text{Ga}_{0.85}\text{As}$  capping layers were grown at 350  $^\circ\text{C}$  via migration-enhanced epitaxy. This was followed by 170 ML of GaAs grown via MBE at 500  $^\circ\text{C}$ . The undoped epitaxial GaAs layer is  $p$  type with a background doping level of  $< 5 \times 10^{14}/\text{cm}^3$ . In such an  $n-i(\text{QD})-n$  structure, the electrons in the active InAs QDs are contributed from the highly doped contact layers.<sup>7,8</sup> Standard photolithography and wet-chemical etching procedures were used to obtain mesas with a diameter of 250  $\mu\text{m}$  and alloyed AuGe/Ni/Au contacts were fabricated. All photocur-

rents (in the form of alternating current) were measured in the normal-incidence configuration using a Fourier transform infrared arrangement and were calibrated with a pyroelectric detector.

A typical cross-sectional transmission electron microscope dark-field image of the QDIP structure shown in Fig. 1(b) indicates that the average QD size of the fifth (top) QD layer is smaller than that of other four QD layers. The macroscopic defect density is  $< 10^8/\text{cm}^2$ . Moreover, atomic-force microscope (AFM) measurements on uncapped reference GaAs(001)/InAs QD samples grown under the same conditions were carried out. The AFM data show that up to the third QD layer an average QD height of 5.6 nm and a density of  $\sim 4 \times 10^{10}/\text{cm}^2$  is maintained. However, by the fifth QD layer a smaller average height of 3.0 nm and a slightly lower density of  $\sim 1 \times 10^{10}/\text{cm}^2$  is found. The reduction of the average QD height and density in the upper layers may be due to the cumulative strain effect at the GaAs spacer surface caused by the strain-relieving InGaAs capping layers.

Figure 2(a) shows 80 K photoluminescence (PL) spectra of the QDIP (five QD layers) as well as a single QD layer sample of  $\text{In}_{0.15}\text{Ga}_{0.85}\text{As}$ -capped GaAs(001)/2.5 ML InAs grown under the same condition. The former has two main peaks at 1.04 eV (1.20  $\mu\text{m}$ ) and 1.11 eV (1.12  $\mu\text{m}$ ). The single QD layer, compared to that of five QD layers, shows two redshifted peaks at 1.02 eV (1.22  $\mu\text{m}$ ) and 1.09 eV (1.14  $\mu\text{m}$ ) but with different relative intensity. In order to identify these PL peaks, we have also measured the PL spectrum of a quantum-well structure, GaAs/1.0 ML InAs/30 ML

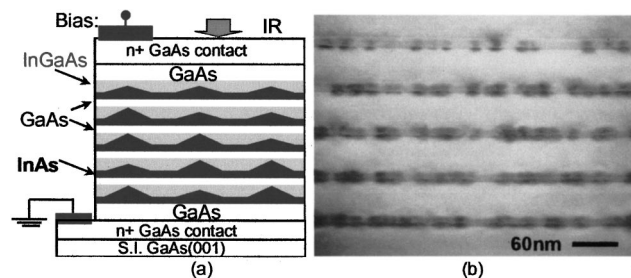


FIG. 1. (a) Schematic of the InGaAs-capped InAs quantum-dot-based infrared photodetector structure. (b) Cross-sectional transmission electron image [ $g=(002)$ , dark field,  $[110]$  azimuth] of InGaAs capped InAs quantum dots.

<sup>a)</sup>Electronic mail: zhonghui@usc.edu

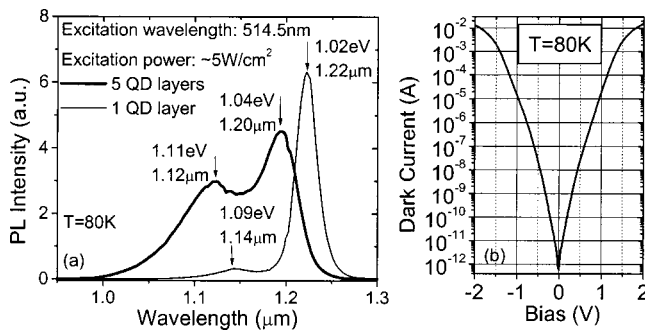


FIG. 2. (a) Photoluminescence spectra of the five and single layer quantum dots; (b) dark current of the quantum-dot infrared photodetector (five quantum-dot layers).

$\text{In}_{0.15}\text{Ga}_{0.85}\text{As}/\text{GaAs}$ , to mimic the absence of the QDs. Our PL measurement indicates the quantum-well ground-state interband photoluminescence peaked at 1.35 eV ( $0.917 \mu\text{m}$ ). Thus, the two main peaks shown in Fig. 2 are due to InAs QD interband (i.e., electron-hole) transitions. Moreover, our systematic studies show that the  $\text{Ar}^+$  excitation power of  $5 \text{ W}/\text{cm}^2$  used for the PL spectra of Fig. 2 is insufficient for significant emission from the excited states of this class of QD ensemble. Therefore, the bimodal PL emission of single and five layer QDs indicates the existence of two types of QDs with different average size and/or shape in a single QD layer and between different QD layers. This is also consistent with the structural data noted above. As it is well established that the ground-state transition energy decreases with increasing QD size,<sup>9</sup> the PL peaks of the QDIP at 1.04 and 1.11 eV can be assigned to large and small QDs, respectively. This assignment is further supported by our recent study of  $\text{In}_{0.15}\text{Ga}_{0.85}\text{As}$ -capped  $\text{GaAs}(001)/2.0 \text{ ML}$  InAs QDs (having average height of  $\sim 3.5 \text{ nm}$ ).<sup>10</sup> Its PL spectrum shows a unimodal peak at 1.13 eV ( $1.10 \mu\text{m}$ ) with a full width at half maximum (FWHM) of 65 meV. This peak is very close to the peak at 1.11 eV of the bimodal emission of the QDIP.

Figure 2(b) shows the dark current (direct current) of this QDIP at 80 K. It is symmetric at negative and positive

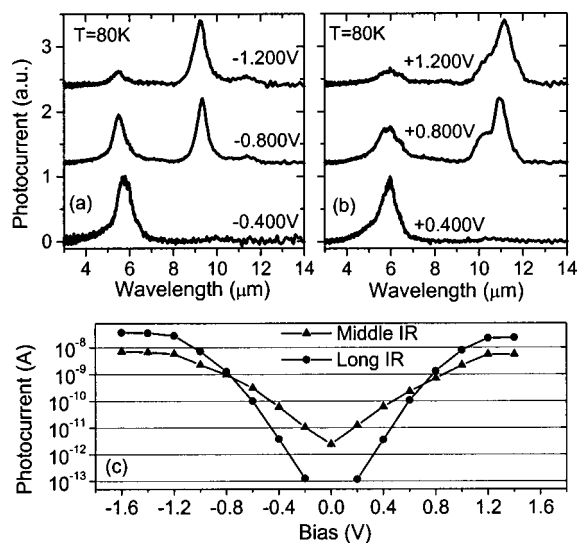


FIG. 3. Intradband photocurrent spectra of the quantum-dot infrared photodetector at 80 K at negative [panel (a)] and positive bias [panel (b)]. Panel (c): Bias dependence of the peak photocurrent at middle- ( $\sim 5.6 \mu\text{m}$ ) and long- ( $\sim 10 \mu\text{m}$ ) infrared wavelengths.

bias. We note that this dark current at 80 K is about two orders of magnitude lower than that found for  $\text{GaAs}(001)/\text{InAs}$  QD-based QDIPs (Ref. 7) with a similar  $n-i-n$  structure. We believe this reduction is mainly due to thicker spacer layers and the deeper binding energies of QD electron ground states in this  $n-i-n$  QDIP, as discussed later.

Figures 3(a) and 3(b) show the middle- and long-wavelength IR intraband photocurrent behavior of the QDIP as a function of negative and positive bias. Note the emergence of a dual-peak response with increasing bias magnitude with a mid-IR peak  $\sim 5.6 \mu\text{m}$  (221 meV) and a long IR peak  $\sim 10 \mu\text{m}$  (124 meV). A voltage-controlled, tunable, dual-wavelength behavior is manifest in the bias dependence of these two photocurrent peak intensities [shown in Fig. 3(c)]. At zero bias, no photocurrent was detected for the long-wavelength ( $\sim 10 \mu\text{m}$ ) radiation, whereas the photocurrent for mid-IR wavelength ( $\sim 5.6 \mu\text{m}$ ) radiation is not zero. This kind of intraband photovoltaic effect (at  $\sim 5.6 \mu\text{m}$ ) is due to the QD intraband-transition-induced dipole moment, which originates from the shape- and inhomogeneous strain-dependent intrinsically asymmetrical potential of the pyramidal QDs.<sup>11</sup> Since larger QDs have lower electron ground state energy, and are thus preferentially occupied at zero bias, we assign the  $\sim 5.6 \mu\text{m}$  photo response to the larger QDs. With increasing bias, the peak intensities of both intraband photocurrents increase rapidly, become comparable at intermediate bias ( $\sim 0.8 \text{ V}$ ), and saturate at high bias. Note that the ratio of the middle- and long-wavelength photocurrents can be varied by up to two orders of magnitude with reasonable change in bias. Significant intraband shift ( $5.5 \mu\text{m}$  to  $6.0 \mu\text{m}$  and  $9.2 \mu\text{m}$  to  $11.2 \mu\text{m}$ ) is observed by varying bias ( $-1.60 \text{ V}$  to  $+1.40 \text{ V}$ ) for both peaks. This intraband peak shift may mainly be contributed by the quantum-confined Stark effect. Importantly, we note that the long-wavelength ( $\sim 9.3 \mu\text{m}$ ) photocurrent peak has a minimum FWHM of 8.2 meV, corresponding to  $\Delta\lambda/\lambda = 6.1\%$ , at a bias of  $-0.800 \text{ V}$ . The extremely narrow, minimum FWHM may be due to collective modes induced by enhanced interdot electron-electron coupling,<sup>12</sup> since the InGaAs capping layer significantly decreases the lateral tunneling barrier between the small QDs with size/shape fluctuation.

The origin of the middle ( $\sim 5.6 \mu\text{m}$ ) and long ( $\sim 10 \mu\text{m}$ ) photoresponse can be understood in terms of the intraband transitions in large and small QDs, respectively, of the  $n-i(2.5 \text{ MLQD})-n$  QDIP structure. This is also strongly supported by our recent studies of  $\text{GaAs}(001)/2.0 \text{ ML}$  InAs/InGaAs QDs, which show predominantly small ( $\sim 3.5 \mu\text{m}$  average height) QDs with a unimodal intraband photoresponse at wavelengths of  $\sim 9 \mu\text{m}$ .<sup>10</sup> Furthermore, the bias dependence of the intraband photocurrent of the  $n-i(2.5 \text{ MLQD})-n$  QDIP [shown in Fig. 3(c)] can be understood as follows. At zero bias, the electron ground-state occupation of small QDs is much lower than that of large QDs at 80 K since their electron ground states are higher by  $\sim 40 \text{ meV}$  (as discussed below). With increasing bias, the electron ground states of the small QDs become increasingly occupied. The gain of photoexcited electrons from the small QDs probably also increases more rapidly with bias than that of the large QDs. At high bias, therefore, the intraband photocurrent of the small QDs exceeds that of the large QDs.

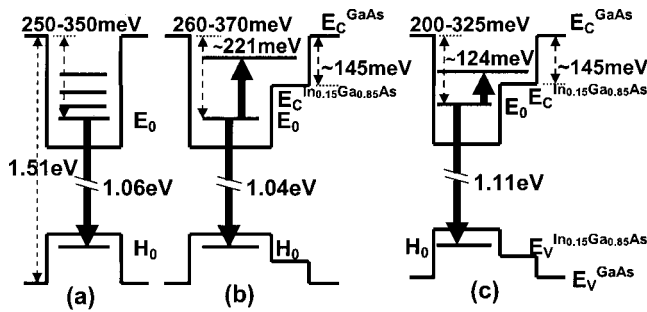


FIG. 4. Energy-level schematic of (a) 3.0 ML, (b) large and (c) small quantum dots.

The issue that naturally arises next is the nature of the states involved in the observed intraband transitions. Regrettably, reliable electronic structure calculations for the type of GaAs(001)/InAs/InGaAs QD structures employed for QDIPs in the current studies do not exist. We estimate upper and lower bounds on the electron ground-state binding energy (with respect to the GaAs conduction-band edge) of small and large QDs based on the following. First, we employ the observed PL transition energies of 1.04 and 1.11 eV (Fig. 2), and the known GaAs band-gap energy of  $\sim 1.51$  eV at 80 K. Second, our previous systematic PL and PL excitation studies on GaAs-capped 3.0 ML InAs QDs indicated an electron ground-state binding energy of  $300 \pm 50$  (i.e., 250–350) meV, as depicted in Fig. 4(a).<sup>13</sup> Third, it is well established that the electron binding energies are significantly higher than those for holes.<sup>9,13–15</sup> And fourth, theoretical results for two GaAs(001)/InAs QDs of different size indicate that the difference of their electron ground-state energies is larger than that of their hole ground-state energies.<sup>14,15</sup> Therefore, as shown in Figs. 4(b) and 4(c), the binding energies of the electron ground states of large and small QDs are in the ranges of 260–370 and 200–325 meV, respectively. Namely, the photocurrent peaks at  $\sim 221$  meV ( $\sim 5.6 \mu\text{m}$ ) and  $\sim 124$  meV ( $\sim 10 \mu\text{m}$ ) are due to transitions from the QD ground state to bound excited states having estimated binding energies as small as 39 and 76 meV, respectively. This, however, is also the energy regime where the InGaAs capping layer regions between the islands, acting as a quantum well, gives rise to its own energy levels arising from the approximately 145 meV conduction-band discontinuity between the GaAs and the strained  $\text{In}_{0.15}\text{Ga}_{0.85}\text{As}$  conduction-band edges.<sup>16,17</sup> The final states of the observed intraband photocurrent peaks at  $\sim 221$  and  $\sim 124$  meV may thus be a mixture of the QD excited states and the InGaAs quantum-well states.

We note that, based upon the available theoretical results<sup>14</sup> for GaAs(001)/InAs/GaAs QDs closest to the large QDs under investigation here, the final states involved in the middle-wavelength ( $\sim 5.6 \mu\text{m}$ ) intraband transitions are not

the first or even second excited bound states, but rather very high bound states (most probably fifth or higher).<sup>13,14</sup> Although the separation between the ground and any given excited electron state decreases with increasing QD size,<sup>9,14,15</sup> our experimental findings of the photocurrent at the lower transition energy ( $\sim 124$  meV) arising from the smaller QDs clearly show the more complex nature of the intraband photocurrent in QD structures due to the convolution, at the minimum, of the transition matrix elements, density of final states, and weighted photocurrent extraction barriers.

In summary, in InGaAs-capped GaAs(001)/InAs QDs we have demonstrated a normal-incidence voltage-controlled tunable middle- ( $\sim 5.6 \mu\text{m}$ ) and long- ( $\sim 10 \mu\text{m}$ ) wavelength IR photoresponse, which is due to bound-to-bound intraband transitions of the large and small QDs, respectively. The two types of QDs of the QDIP structure exist in the single QD layer and between different QD layers. Our results suggest good potential for InAs/GaAs QDs in multicolor normal-incidence IR sensor and imaging applications.

This work was supported by the DoD Multidisciplinary University Research Initiative (MURI) program administered by AFOSR under Grant No. F49620-98-1-0474.

<sup>1</sup>Y. H. Zhang, D. S. Jiang, J. B. Xia, L. Q. Cui, C. Y. Song, Z. Q. Zhou, and W. K. Ge, *Appl. Phys. Lett.* **68**, 2114 (1996), and references therein.

<sup>2</sup>D. Bimberg, M. Grundmann, and N. Ledentsov, *Quantum Dot Heterostructures* (Wiley, New York, 1998).

<sup>3</sup>V. Ryzhii, *Semicond. Sci. Technol.* **11**, 759 (1996).

<sup>4</sup>H. Benisty, C. M. Sotomayer-Torrès, and C. Weisbuch, *Phys. Rev. B* **44**, 10945 (1991).

<sup>5</sup>D. Pan, E. Towe, and S. Kennerly, *Appl. Phys. Lett.* **73**, 1937 (1998); **75**, 2719 (1999); **76**, 3301 (2000).

<sup>6</sup>S. Maimon, E. Finkman, G. Bahir, S. E. Schacham, J. M. Garcia, and P. M. Petroff, *Appl. Phys. Lett.* **73**, 2003 (1998).

<sup>7</sup>Z. H. Chen, O. Baklenov, E. T. Kim, I. Mukhametzhanov, J. Tie, A. Madhukar, Z. Ye, and J. C. Campbell, *J. Appl. Phys.* **89**, 4558 (2001);

<sup>8</sup>Z. H. Chen, E. T. Kim, and A. Madhukar, *J. Vac. Sci. Technol. B* (in press).

<sup>9</sup>R. Heitz, O. Stier, I. Mukhametzhanov, A. Madhukar, and D. Bimberg, *Phys. Rev. B* **62**, 11017 (2000).

<sup>10</sup>E. T. Kim, Z. H. Chen, and A. Madhukar, *Appl. Phys. Lett.* **79**, 3341 (2001).

<sup>11</sup>Z. H. Chen, E. T. Kim, and A. Madhukar, *Appl. Phys. Lett.* (in press).

<sup>12</sup>U. Merkt, *Phys. Rev. Lett.* **76**, 1134 (1996); C. Metzner and G. H. Döhler, *Phys. Rev. B* **60**, 11005 (1999).

<sup>13</sup>I. Mukhametzhanov, Z. H. Chen, O. Baklenov, E. T. Kim, and A. Madhukar, *Phys. Status Solidi B* **224**, 697 (2001).

<sup>14</sup>O. Stier, M. Grundmann, and D. Bimberg, *Phys. Rev. B* **59**, 5688 (1999); O. Stier, Ph.D. dissertation, Technical University Berlin, Berlin, Germany (2001), p. 55.

<sup>15</sup>L. W. Wang, J. Kim, and A. Zunger, *Phys. Rev. B* **59**, 5678 (1999); S. J. Sun, and Y. C. Chang, *Phys. Rev. B* **62**, 13631 (2001).

<sup>16</sup>G. Ji, D. Huang, U. K. Reddy, T. S. Henderson, R. Houvrou, and H. Morkoc, *J. Appl. Phys.* **62**, 3366 (1987).

<sup>17</sup>D. J. Arent, K. Deneffe, C. Van Hoof, J. DeBoeck, and G. Borghs, *J. Appl. Phys.* **66**, 1739 (1989).